Synthesis and Bio-adsorptive Properties of Large-Pore Periodic Mesoporous Organosilica Rods

S. Z. Qiao,[†] C. Z. Yu,[†,‡] W. Xing,[†,§] Q. H. Hu,[†] H. Djojoputro,[†] and G. Q. Lu*[,†]

ARC Centre for Functional Nanomaterials, School of Engineering, The University of Queensland, St Lucia, QLD 4072, Australia, Department of Chemistry and Shanghai Key Laboratory of Molecular Catalysis and Innovative Materials, Fudan University, Shanghai 200433, P.R. China, and State Key Laboratory for Heavy Oil Processing, Key Laboratory of Catalysis, CNPC, University of Petroleum, Dongying 257061, China

Received August 3, 2005. Revised Manuscript Received September 29, 2005

Highly ordered large-pore periodic mesoporous organosilica (PMO) with a rodlike morphology was successfully synthesized at low acid concentrations and in the presence of inorganic salt using triblock copolymer P123 as a template. The inorganic salt can not only promote the formation of highly ordered mesoporous structure but also control the morphology of PMO materials. The adsorption of bovine heart cytochrome c (cyt c) on PMO was studied at different ionic strengths and pHs by comparing with the adsorption on pure silica materials with similar morphology and pore structure. The results show that the adsorbed amount reaches the maximum around the isoelectric point of cyt c and the PMO materials do not have higher adsorbed capacity than SBA-15 silica. The specific adsorption amounts of cyt c on PMO or pure silica decrease as ionic strengths increase at all pH conditions. Our results directly support the conclusion that the electrostatic interaction between cyt c and PMO/pure silica surface is more dominant than hydrophobic forces in the bioadsorption of cyt c.

1. Introduction

Synthesis of large-pore PMOs with controlled morphology is extremely important for potential applications in catalysis, adsorption, separation, chromatography, and sensors.[1−5] To date, PMOs have been prepared using various bridged organic groups.[6−30] Most studies have focused on the synthesis of small-pore PMOs (<5 nm) using cationic surfactants as templates in alkaline media[6−18] or polyoxyethylene nonionic surfactants as templates in acidic solution.[19−23] The large-pore PMOs (5−10 nm) have also been synthesized using triblock copolymers as templates under strongly acidic conditions; however, they usually exhibited poorly ordered mesostructures.[24−26] Very recently, a low-acidity synthesis approach has been proposed to produce PMO materials but the highly ordered mesostructure can only be produced in a very small range of acid concentration (0.016−0.08 M HCl).[27,28] An inorganic salt-assisted pathway has also been proposed at high acidity to produce ordered PMOs.[26,29,30] In this route, the use of high acid concentration is compensated by a very high concentra-

* To whom correspondence should be addressed. E-mail: maxlu@uq.edu.au. Phone: +61 7 33653885. Fax: +61 7 33656074.
[†] The University of Queensland.
[‡] Fudan University.
[§] University of Petroleum.

(1) Wight, A. P.; Davis, M. E. *Chem. Rev.* **2002**, *102*, 3589.
(2) Baleizao, C.; Gigante, B.; Das, D.; Alvaro, M.; Garcia, H.; Corma, A. *Chem. Commun.* **2003**, 1860.
(3) Burleigh, M. C.; Markowitz, M. A.; Spector, M. S.; Gaber, B. P. *Environ. Sci. Technol.* **2002**, *36*, 2515.
(4) Burleigh, M. C.; Dai, S.; Hagaman, E. W.; Lin, J. S. *Chem. Mater.* **2001**, *13*, 2537.
(5) Yang, Q. H.; Kapoor, M. P.; Inagaki, S. *J. Am. Chem. Soc.* **2002**, *124*, 9694.
(6) Asefa, T.; MacLachlan, M. J.; Grondey, H.; Coombs, N.; Ozin, G. A. *Angew. Chem., Int. Ed.* **2000**, *39*, 1808.
(7) Inagaki, S.; Guan, S.; Fukushima, Y.; Ohsuna, T.; Terasaki, O. *J. Am. Chem. Soc.* **1999**, *121*, 9611.
(8) Melde, B. J.; Holland, B. T.; Blanford, C. F.; Stein, A. *Chem. Mater.* **1999**, *11*, 3302.
(9) Sayari, A.; Hamoudi, S.; Yang, Y.; Moudrakovski, I. L.; Ripmeester, J. R. *Chem. Mater.* **2000**, *12*, 3857.
(10) Lu, Y. F.; Fan, H. Y.; Doke, N.; Loy, D. A.; Assink, R. A.; LaVan, D. A.; Brinker, C. J. *J. Am. Chem. Soc.* **2000**, *122*, 5258.
(11) Asefa, T.; MacLachan, M. J.; Coombs, N.; Ozin, G. A. *Nature* **1999**, *402*, 867.
(12) Inagaki, S.; Guan, S.; Ohsuna, T.; Terasaki, O. *Nature* **2002**, *416*, 304.
(13) Yoshina-Ishii, C.; Asefa, T.; Coombs, N.; MacLachlan, M. J.; Ozin, G. A. *Chem. Commun.* **1999**, 2539.
(14) Morell, J.; Wolter, G.; Froba, M. *Chem. Mater.* **2005**, *17*, 804.
(15) Kapoor, M. P.; Yang, Q. H.; Inagaki, S. *J. Am. Chem. Soc.* **2002**, *124*, 15176.
(16) Landskron, K.; Hatton, B. D.; Perovic, D. D.; Ozin, G. A. *Science* **2003**, *302*, 266.
(17) Hamoudi, S.; Yang, Y.; Moudrakovski, I. L.; Lang, S.; Sayari, A. *J. Phys. Chem. B* **2001**, *105*, 9118.
(18) Corriu, R. J. P.; Mehdi, A.; Reye, C.; Thieuleux, C. *Chem. Commun.* **2002**, 1382.
(19) Burleigh, M. C.; Markowitz, M. A.; Jayasundera, S.; Spector, M. S.; Thomas, C. W.; Gaber, B. P. *J. Phys. Chem. B* **2003**, *107*, 12628.
(20) Olkhovyk, O.; Jaroniec, M. *J. Am. Chem. Soc.* **2005**, *127*, 60.
(21) Sayari, A.; Yang, Y. *Chem. Commun.* **2002**, 2582.
(22) Hamoudi, S.; Kaliaguine, S. *Chem. Commun.* **2002**, 2118.
(23) Burleigh, M. C.; Markowitz, M. A.; Spector, M. S.; Gaber, B. P. *J. Phys. Chem. B* **2002**, *106*, 9712.
(24) Zhu, H. G.; Jones, D. J.; Zajac, J.; Roziere, J.; Dutartre, R. *Chem. Commun.* **2001**, 2568.
(25) Muth, O.; Schellbach, C.; Froba, M. *Chem. Commun.* **2001**, 2032.
(26) Guo, W. P.; Park, J. Y.; Oh, M. O.; Jeong, H. W.; Cho, W. J.; Kim, I.; Ha, C. S. *Chem. Mater.* **2003**, *15*, 2295.
(27) Bao, X. Y.; Zhao, X. S.; Li, X.; Chia, P. A.; Li, J. *J. Phys. Chem. B* **2004**, *108*, 4684.
(28) Bao, X. Y.; Zhao, X. S.; Qiao, S. Z.; Bhatia, S. K. *J. Phys. Chem. B* **2004**, *108*, 16441.
(29) Guo, W. P.; Kim, I.; Ha, C. S. *Chem. Commun.* **2003**, 2692.
(30) Zhao, L.; Zhu, G. S.; Zhang, D. L.; Di, Y.; Chen, Y.; Terasaki, O.; Qiu, S. L. *J. Phys. Chem. B* **2005**, *109*, 764.

10.1021/cm051735b CCC: $30.25
Published on Web 11/01/2005

tion of inorganic salts to obtain highly ordered PMOs. Under such conditions, the sol−gel kinetics of organosilica precursors is too fast[31] and the induction time for precipitation is too short to have good control over the morphology of PMO particles.[32] A recent study revealed that rodlike SBA-15 pure silica materials possessed much better immobilization behaviors for enzymes than conventional SBA-15 materials.[33] However, there has been no report on successful synthesis of large-pore PMOs with uniform rodlike morphology so far, although a few reports have described the preparation of PMOs with well-defined morphologies, such as spheres,[34−36] nonuniform curved rod,[37,38] dodecahedron,[9,39] decaoctahedron,[34,40] and films.[10,41] Previous studies have shown that inorganic salts play an important role in controlling the morphology as well as the mesostructure of pure silicas.[32,42] It is expected that the simultaneous use of low acidity and inorganic salts during the synthesis may give rise to highly ordered PMOs with controlled morphology, promising for many biological applications.

The electrostatic and hydrophobic interactions are two types of driving forces in the immobilization of biomolecules into porous hosts. The influencing factors may include the experimental conditions such as the ionic strength,[43] temperature,[44] pH[43,45−47] of the buffer solutions, and the material properties such as the size of enzymes and nanopores,[48] the composition (silica and carbon,[45,49] organic-grafted silica[50,51]), mesostructure,[52] and morphology[33,44] of mesoporous materials. Previous study on the adsorption of cytochrome c (cyt c) on pure silica materials showed that strong electrostatic interactions between the surface silanol groups and the surface charge of cyt c molecules was a critical factor;[46,52] however, in another report, Deere et al.[43] suggested that hydrophobic interactions rather than electrostatic interactions dominated the adsorption of cyt c onto some silica materials (commercial Kiesegel silica). The effect of pH on the adsorption of cyt c on mesoporous carbon and silicas has been studied very recently.[45,49] The results revealed that the adsorption of cyt c was determined by electrostatic and hydrophobic interactions as well as the cohesive attraction and repulsion of the amino acids present in the cyt c molecules simultaneously. To better understand the molecular interactions, changing ionic strength is a convenient approach because it can increase or decrease the adsorbed amount of proteins when the dominant interaction is hydrophobic or electrostatic force, respectively.[53] Considering the difference in the wall nature of pure mesostructured silica and PMOs, comparison of the bio-adsorption behavior between the two types of materials would provide more information for studying the driving force in a bio-immobilization process. Importantly, because both the pore structure and the morphology of mesoporous materials may have significant influence on their bio-adsorption behavior,[33,34,52] it is crucial to keep the similar mesostructure and macrostructure of both materials during study for a reasonable comparison. Similar investigation under this premise has not been reported so far in the literature.

This paper reports the successful synthesis of highly ordered PMOs with uniform rodlike morphology (1−2 μm in length) in low-acid concentrations assisted by inorganic salt. The adsorption isotherms of cyt c on both PMO and pure silica SBA-15 with controlled mesostructure and morphology are presented and compared. The effect of ionic strength and pH on the adsorption capacity is quantitatively determined to explain the interaction between biological molecules and the surface of PMO materials.

2. Experimental Section

2.1. Synthesis of Materials. Highly ordered large-pore rodlike PMOs were synthesized by using 1,2-bis(trimethoxysilyl)ethane (BTME, 96%, Aldrich) as precursor and poly(ethylene oxides)-*b*-poly(propylene oxides)-*b*-poly(ethylene oxides) triblock copolymer $EO_{20}PO_{70}EO_{20}$ (Pluronic P123, Aldrich) as a structure-directing agent in the presence of inorganic salt (KCl, 99.5%, AnalaR, Australia). In a typical synthesis, 0.5 g of P123 and 1.49 g (1M) of KCl were dissolved in 20 g of 0.167 M HCl at 38 °C. Then 0.70 g of BTME was added to the solution under stirring. The final reactant molar composition was 0.035:8:1.34:444:1.0 P123:KCl:HCl:H_2O:BTME. After being stirred for 10 min, the solution was kept in static conditions at the same temperature for 24 h. The mixture was transferred into an autoclave and heated at 100 °C for another 24 h. The solid was collected by filtration and dried at room temperature in air. The resulting powders were washed by deionized water and extracted by refluxing with ethanol for 8 h to remove the templates. The SBA-15 silica rod used in this study was prepared according to the method reported by previous papers[32,42] except that the surfactants were extracted by ethanol instead of being calcined.

2.2. Adsorption of Cytochrome c. For cyt c adsorption, about 15 mg of the mesoporous material was suspended in 4 mL of 10 mM buffer solution (pH = 7.0 potassium phosphate buffer and pH

(31) Brinker, C. J.; Scherer, G. W. *Sol−gel science: the physics and chemistry of sol−gel processing*; Academic Press: New York, 1990.
(32) Yu, C. Z.; Fan, J.; Tian, B. Z.; Zhao, D. Y. *Chem. Mater.* **2004**, *16*, 889.
(33) Fan, J.; Lei, J.; Wang, L. M.; Yu, C. Z.; Tu, B.; Zhao, D. Y. *Chem. Commun.* **2003**, 2140.
(34) Kim, D. J.; Chung, J. S.; Ahn, W. S.; Kam, G. W.; Cheong, W. J. *Chem. Lett.* **2004**, *33*, 422.
(35) Rebbin, V.; Jakubowski, M.; Potz, S.; Froba, M. *Microporous Mesoporous Mater.* **2004**, *72*, 99.
(36) Kapoor, M. P.; Inagaki, S. *Chem. Lett.* **2004**, *33*, 88.
(37) Goto, Y.; Inagaki, S. *Chem. Commun.* **2002**, 2410.
(38) Wahab, M. A.; Imae, I.; Kawakami, Y.; Ha, C. S. *Chem. Mater.* **2005**, *17*, 2165.
(39) Kapoor, M. P.; Inagaki, S. *Chem. Mater.* **2002**, *14*, 3509.
(40) Guan, S.; Inagaki, S.; Ohsuna, T.; Terasaki, O. *J. Am. Chem. Soc.* **2000**, *122*, 5660.
(41) Dag, O.; Yoshina-Ishii, C.; Asefa, T.; MacLachlan, M. J.; Grondey, H.; Coombs, N.; Ozin, G. A. *Adv. Funct. Mater.* **2001**, *11*, 213.
(42) Yu, C. Z.; Fan, J.; Tian, B. Z.; Zhao, D. Y.; Stucky, G. D. *Adv. Mater.* **2002**, *14*, 1742.
(43) Deere, J.; Magner, E.; Wall, J. G.; Hodnett, B. K. *J. Phys. Chem. B* **2002**, *106*, 7340.
(44) Lei, J.; Fan, J.; Yu, C. Z.; Zhang, L. Y.; Jiang, S. Y.; Tu, B.; Zhao, D. Y. *Microporous Mesoporous Mater.* **2004**, *73*, 121.
(45) Vinu, A.; Murugesan, V.; Tangermann, O.; Hartmann, M. *Chem. Mater.* **2004**, *16*, 3056.
(46) Diaz, J. F.; Balkus, K. J. *J. Mol. Catal. B-Enzym.* **1996**, *2*, 115.
(47) Han, Y. J.; Watson, J. T.; Stucky, G. D.; Butler, A. *J. Mol. Catal. B-Enzym.* **2002**, *17*, 1.
(48) Lei, C. H.; Shin, Y. S.; Liu, J.; Ackerman, E. J. *J. Am. Chem. Soc.* **2002**, *124*, 11242.
(49) Vinu, A.; Streb, C.; Murugesan, V.; Hartmann, M. *J. Phys. Chem. B* **2003**, *107*, 8297.
(50) Yiu, H. H. P.; Wright, P. A. *J. Mater. Chem.* **2005**, *15*, 3690.
(51) Hartmann, M. *Chem. Mater.* **2005**, *17*, 4577.
(52) Washmon-Kriel, L.; Jimenez, V. L.; Balkus, K. J. *J. Mol. Catal. B-Enzym.* **2000**, *10*, 453.
(53) Zhang, S. P.; Sun, Y. *Biotechnol. Bioeng.* **2001**, *75*, 710.

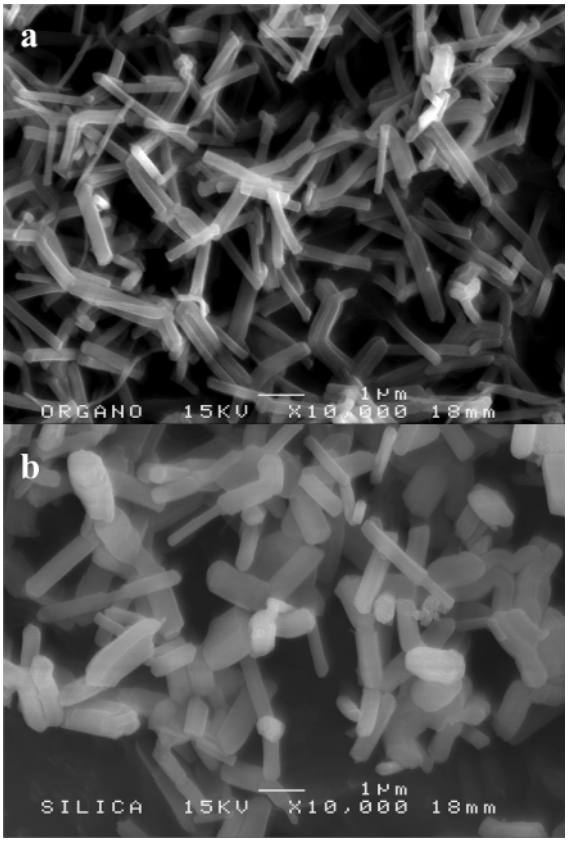

Figure 1. SEM images of surfactant-extracted (a) PMO and (b) SBA-15 silica materials with rodlike morphology. SEM images were collected by a JSM 6400F field emission microscope using 15 kV acceleration voltages.

= 9.6 sodium bicarbonate buffer) with different cyt c (95%, Sigma) concentration (from 0.12 to 3.5 g/L). The ionic strength of buffer solution was adjusted by adding different amounts of NaCl. The resulting mixture was placed into a water bath controlled at 30 °C and continuously shaken for 96 h, which was demonstrated to be long enough to reach the adsorption equilibrium in our study and literature.[45,49] The suspension was then centrifuged and the supernatant analyzed by ultraviolet absorbance at 409 nm to determine the adsorption amount of cyt c according to the following equation:

$$q = \frac{V_0(C_0 - C)}{W} \quad (1)$$

where q is the equilibrium adsorbed amount in the particles, C_0 and C are the protein concentrations at initial and equilibrium solution, respectively, V_0 is the volume of the initial protein solution, and w is the weight of the adsorbent.

3. Results and Discussions

Figure 1 shows the scanning electron microscopy (SEM) images of surfactant-extracted PMOs and SBA-15 pure silica. It can be observed that the use of low-acid concentration and inorganic salts results in straight rodlike morphologies (Figure 1a). Compared with SBA-15 silica (Figure 1b) synthesized at 38 °C with the addition of 0.5 M KCl, the PMO materials have relatively uniform rodlike morphology with 1−2 μm length. The transmission electron microscopy (TEM) images viewed along different directions of PMO samples further confirm the highly ordered hexagonal pore structure with one-dimensional (1-D) channels parallel to the long axes of the rods (Figure 2). X-ray diffraction (XRD)

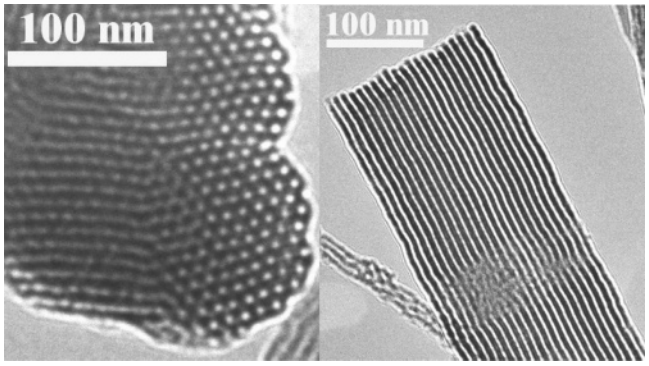

Figure 2. TEM images of surfactant-extracted PMO. TEM images were obtained on a JEM 2010 operating at an acceleration voltage of 200 kV.

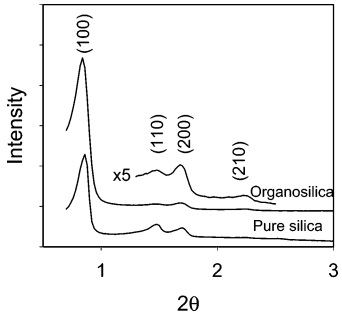

Figure 3. XRD patterns of surfactant-extracted PMO and SBA-15 silica materials. The powder XRD measurements were carried out on a Bruker D8 Advance diffractometer using Cu Kα radiation.

Table 1. Structural Parameters of Pure Silica (SBA-15) and Organosilica Samples (PMO)[a]

sample	d_{100} (nm)	a (nm)	S_{BET} (m^2/g)	V (cm^3/g)	d_{ad} (nm)	d_{de} (nm)
PMO	10.51	12.13	762.9	0.988	7.58	5.95
SBA-15	10.26	11.85	695.6	1.189	8.77	6.98

[a] The unit cell parameters, a, were determined from the interplanar spacings of the (100) planes using the formula of $a = 2d_{100}/\sqrt{3}$; pore sizes, d_{ad} and d_{de}, were calculated from nitrogen sorption data based on the BJH model from adsorption and desorption branches, respectively; S is the BET surface area; and V is the total pore volume estimated at a relative pressure of 0.99.

patterns of surfactant-extracted PMO and SBA-15 pure silica are shown in Figure 3. The XRD peaks, assigned to the (100), (110), (200), and (210) diffractions, reflect a two-dimensional hexagonal mesostructure with a space group of *p6mm*. The high peak intensity and resolution of (110), (200), and (210) can be attributed to the long-range regularity of PMO rods because of the use of low-acid concentration in the presence of salt. The unit cell parameters of PMO and SBA-15 materials are 12.1 and 11.85 nm, respectively, and the results are listed in Table 1.

The nitrogen sorption isotherms of PMO and SBA-15 silica, shown in Figure 4, are of type IV with type H1 hysteresis loops which are characteristic of mesoporous materials with 1-D cylindrical channels. The narrow and sharp pore-size distribution curves (inset of Figure 4) reveal that PMO and SBA-15 silica materials have highly uniform pore size. The pore sizes, calculated from the adsorption and desorption branches of the isotherm by the BJH method, pore volumes, and BET surface areas are also summarized in Table 1. Although high salt concentration (1 M) was utilized in the synthesis process, PMO still had a large BET surface area of 762.9 m^2/g and a large pore volume of 0.988 cm^3/g.

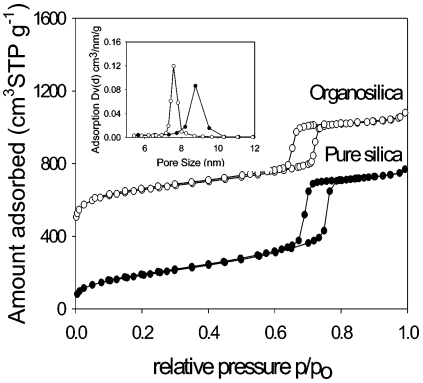

Figure 4. Nitrogen adsorption−desorption isotherms and pore size distribution curves (inset) of surfactant-extracted organosilica and pure silica. N_2 adsorption was measured on a Quanta Autosorb-1 system at 77 K and the samples were degassed at 373 K overnight before measurement. The pore size distributions were determined from the adsorption branches of the isotherms by the BJH model.

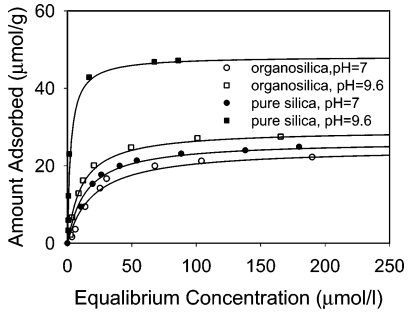

Figure 5. Adsorption isotherm of cytochrome c on pure silica and organosilica at different solution pH. The solid lines are fitting results of the Langmuir equation.

It can be seen that the PMO and SBA-15 silica materials have similar pore sizes, pore volumes, and surface areas, which is important in comparing biological adsorption capacity of PMO and SBA-15 silica.

Our study reveals that the highly ordered rodlike PMOs can be synthesized by carefully choosing the acidity and the concentration of inorganic salts simultaneously. The adding of inorganic salt can greatly expand the acidity range (0.03−1.5 M HCl) in which ordered mesostructures of PMOs can be obtained; however, exclusively rodlike morphology can only be synthesized in a narrow range of acid (0.167−0.25 M HCl) and salt (0.5−1.0 M KCl) concentrations (at 40 °C). The influence of acidity, salt concentration, temperature, and the reactant molar ratio upon the mesostructure and macrostructure of PMOs will be reported in details elsewhere.

The isotherms of cyt c adsorption on SBA-15 pure silica and PMO with rodlike morphologies at 30 °C and different pH values are shown in Figure 5. A low buffer concentration (10 mM) was used in this study to reduce the effect of ionic strength on adsorption. All isotherms show a sharp initial rise and then reach maximum adsorption amounts (plateau) at about 50−200 μmol/L equilibrium concentration, suggesting that isotherms are of Langmuir type. The solid lines are the fitting results of the Langmuir model using a nonlinear regression method, which shows that the model fitted the data well. It can be seen that the equilibrium adsorbed amount on SBA-15 silica is significantly affected by solution pH and the maximum adsorbed amount at pH 9.6 (near the isoelectric point (pI) of cyt c, 9.8[45]) is 48.24

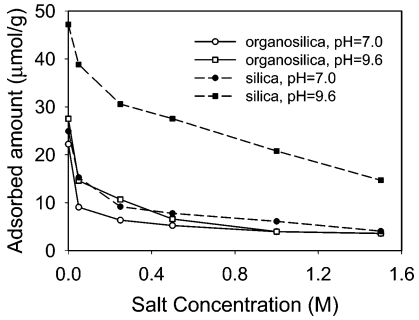

Figure 6. Effect of salt concentration on the adsorption capacity of cytochrome *c* on organosilica and pure silica at different solution pH.

μmol/g, which is 2 times larger than the adsorbed amount of 24.9 μmol/g at pH 7.0. Moreover, this maximum adsorption amount at 30 °C is larger than the maximum amount of 41.5 μmol/g of cyt c adsorption on conventional SBA-15 at the same pH reported by other investigators.[45] The reason is probably that the SBA-15 with a rodlike morphology possesses more ordered mesoporous structure and more entrance spaces to entrap enzymes than conventional SBA-15. In contrast, it can be seen that the pH has a small influence upon the adsorption isotherm of cyt c in PMO. The maximum adsorbed amount of cyt c in PMO at pH 9.6 (27.53 μmol/g) is slightly larger than that at pH 7.0 (22.22 μmol/g). It is also important to note that the maximum adsorbed amount for pure silica at pH 9.6 is much larger than that for PMO at the same pH, while at pH 7.0 the maximum amount for pure silica is only slightly larger than that for PMO.

Figure 6 shows the effect of ionic strength on cyt c adsorption on SBA-15 and PMO materials. It can be seen that the specific adsorption amounts decrease as ionic strengths (salt concentration) increase both for SBA-15 silica and for PMO at all pH conditions in this study. The specific adsorption amount of cyt c on SBA-15 at a given salt concentration is larger than that on PMO at the same pH. When the salt concentration is increased from 0 to 1.5 M, the specific adsorption amounts are decreased for pure silica vs PMO by 32.51 vs 23.93 μmol/g and 20.83 vs 18.65 μmol/L at pH 9.6 and 7.0, respectively. The increasing ionic strength has a larger and pH-sensitive influence upon the maximum adsorption amount of cyt c on pure silica, but a relatively smaller and pH-independent influence on PMO.

The adsorption of cyt c on silica or organosilica materials is determined by several factors when the adsorbent materials have similar mesostructure and macrostructure as those in our study. These include electrostatic interactions between the surface silanol groups and the surface charge of the amino acid residues on the surface of cyt c, the hydrophobic interactions between the organic groups inside the channel walls and nonpolar side chains of the amino acids residues on the surface of cyt c, and the interaction between the amino acids present in the neighboring cyt c molecules in the adsorbents.[45,49] The expansion and contraction of the molecular diameter of the proteins at different pH also affect the adsorbed amount significantly.[49] When the solution pH 9.6 is near the isoelectric point (pI) 9.8 of cyt c, the net charge of cyt c is near zero. Thus, the electrostatic repulsion between the amino acid residues on the surface of cyt c molecules is

very small; the cyt c molecules can pack closely within the adsorbent (the size of cyt c is 2.6 × 3.2 × 3.0 nm,[45] smaller than the pore sizes of silica or organosilica) and the monolayer adsorbed capacity is large near the pI of cyt c. However, although the overall net charge for proteins is zero at pI, there still exists positively (or negatively) charged regions on the protein surface and the negatively charged silanols has strong electrostatic interaction with polar and positively charged regions of the cyt c molecules. Although hydrophobic interaction is considered as more important near pI, it is believed to be much weaker than electrostatic interaction forces.[54] It should be noted that, at pH = 9.6, where the repulsion between cyt c molecules is small, the possibility of coagulation between cyt c molecules must be ruled out so that these biomolecules are indeed adsorbed into the mesoporous host. This was confirmed by a blank experiment (not adsorbent added): after the cyt c solution was continuously shaken for 96 h at pH = 9.6, the absorbance change is less than 1.0%. Moreover, the fact that SBA-15 silica rods possess ~2 times larger maximum adsorption amounts of cyt c than PMOs at pH 9.6 also indicates that it is the adsorption other than coagulation that is responsible for such difference; otherwise, the coagulation could result in similar "adsorbed capacities" for both adsorbents.

Our results directly lead to the conclusion that the electrostatic interaction between cyt c and PMO/SBA-15 hosts is a much more important force than the hydrophobic interactions. First, the influence of ionic strength upon the maximum adsorption amount supports this conclusion: the decrease in adsorbed amount of proteins with increasing ionic strength suggests that the overall interaction is dominated by the electrostatic force.[53] Second, the fact that SBA-15 silica rods possess much larger maximum adsorption amounts than PMOs at pH 9.6 also supports this conclusion because there exist more hydroxyl groups on the silica surface and stronger electrostatic interaction with SBA-15 silica. This is easily understood by zeta-potential data measured at different adsorption conditions. Zeta-potentials for SBA-15 vs PMO in the buffer solution are −29.9 vs −20.4 mV and −16.2 vs −12.7 mV at pH 9.6 and 7.0, respectively. SBA-15 has larger numbers of negative charges than PMO at both pH values, and both adsorbents have significantly more negative charges at pH 9.6 than at pH 7.0. Although cyt c is highly charged at pH 7.0 compared to that at pH 9.6, the electrostatic forces from the side of the adsorbent substrate may contribute more significantly to adsorption of cyt c based on the analysis of adsorption (Figure 5) and zeta-potential data. Third, when comparing the maximum adsorption capacities of silica or PMO at different pH values, it is easy to explain lower maximum adsorption amount at pH 7.0 than at pH 9.6 by considering the electrostatic repulsions between neighboring positively charged cyt c molecules (requiring more space) as discussed above. The above experimental observations also imply that the hydrophobic interaction cannot be neglected and might be responsible for the similar adsorption capacity of PMO with that of SBA-15 at pH 7.0 (Figure 5); the charge density of silanols is lower at this pH than at pH 9.6 and therefore the electrostatic attraction is less strong. Finally, this understanding may explain the influence of ionic strength upon the adsorption amount for silica vs PMO at different pHs quite well (Figure 6): when the electrostatic interaction is the strongest among all cases (pH 9.6 for silica), the specific adsorption amount is decreased to the largest extent when the same ionic strength is employed, further confirming our conclusion that the electrostatic interaction between cyt c and mesoporous hosts is the dominant force during the bio-sorption process.

4. Conclusion

In summary, highly ordered rodlike large-pore PMO has been successfully synthesized at low-acid concentration assisted by inorganic salt using triblock copolymer P123 as a template. The inorganic salt can not only promote the formation of highly ordered mesoporous structure but also control the morphology of PMO materials. The bio-adsorption studies show that the adsorbed amount reaches the maximum around the isoelectric point of cyt c and the PMO materials do not have a higher adsorbed capacity than SBA-15 silica at both the isoelectric point of cyt c and pH = 7.0. Our results directly support the conclusion that the hydrophobic force is weak compared to the electrostatic interaction for the bio-sorption of cyt c in both nanoporous materials.

Acknowledgment. This work was financially supported by the Australian Research Council (ARC) through the Discovery Project program (DP0452461) and UQ through Early Career Researcher Grant (2004001423), and also as part of the activities of the ARC Centre for Functional Nanomaterials funded by ARC under the ARC Centres of Excellence Program. S.Z.Q. and C.Z.Y. are also grateful to the ARC for an APD fellowship and international fellowship (LX0560166), respectively.

CM051735B

(54) Matsui, M.; Kiyozumi, Y.; Yamamoto, T.; Mizushina, Y.; Mizukami, F.; Sakaguchi, K. *Chem.-Eur. J.* **2001**, *7*, 1555.